Tian et al., http://www.jgp.org/cgi/content/full/jgp.201511363/DC1

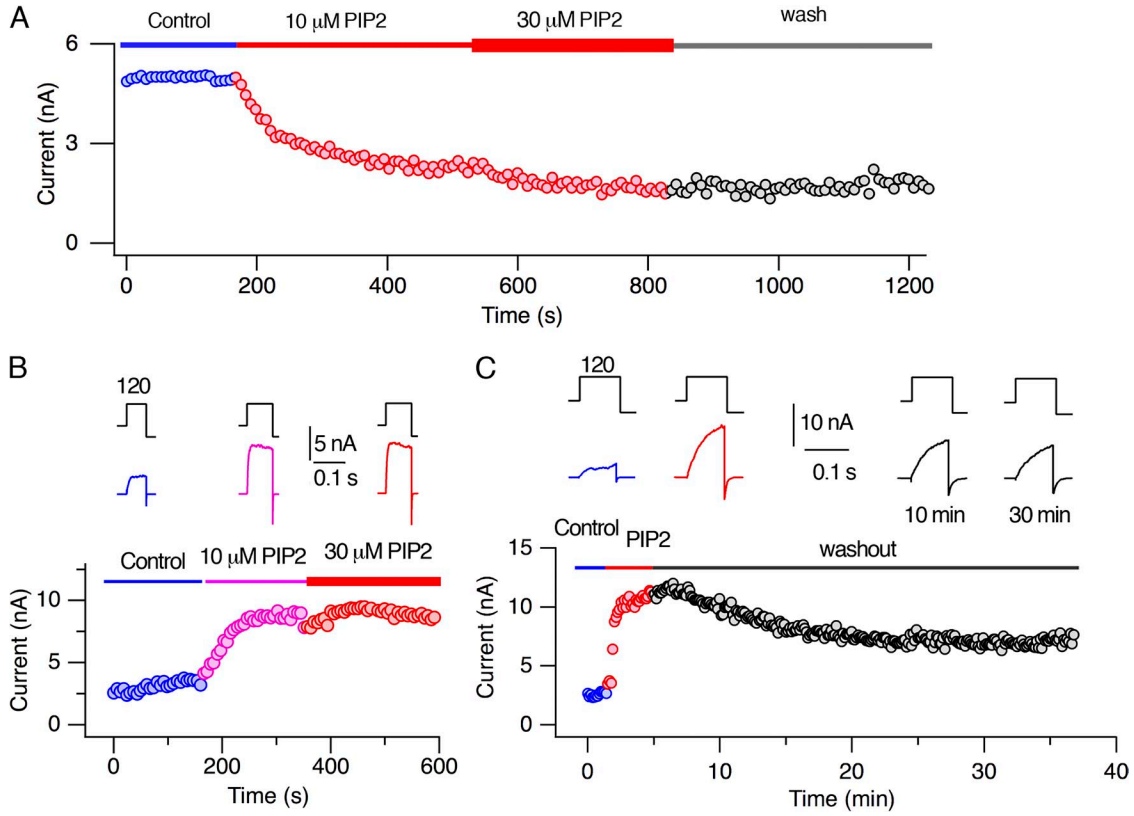

Figure S1. Concentration dependence and slow reversibility of the PIP_2 action. (A) Peak outward current size at 150 mV as a function of time before the application of PIP_2 (blue), in the presence of 10 and 30 μM PIP_2 (red), and after washout of PIP_2 (black) in Slo1 channels. (B) Current-enhancing effect of PIP_2 in Slo1+ β1 is functionally saturated at 10 μM. Representative currents at 120 mV before and after the application of 10 and 30 μM PIP_2 (top) and peak outward current size at 120 mV (bottom). (C) Illustrative currents (top) and peak outward current size (bottom) recorded from Slo1+ β1 before the application of PIP_2 (blue), in the presence of 10 μM PIP_2 (red), and after washout of PIP_2 (black). Currents were recorded without Ca^{2+}.

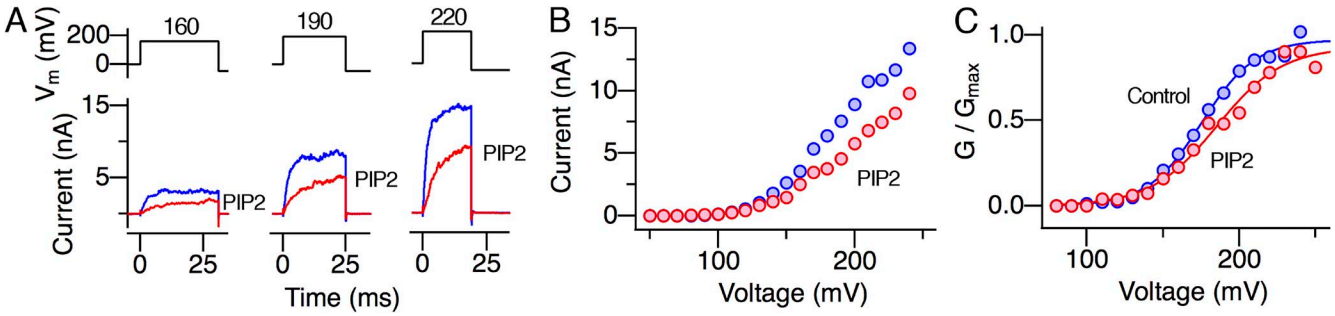

Figure S2. Inhibitory effect of PIP_2 on Slo1 channels expressed in *Xenopus* oocytes. (A) Representative currents through Slo1 from a patch taken from a *Xenopus* oocyte before (blue) and after (red) the application of 10 μM PIP_2. (B) Representative peak I-V curves from Slo1 expressed in a *Xenopus* oocyte before (blue) and after (red) the application of 10 μM PIP_2. (C) G-V curves from Slo1 expressed in *Xenopus* oocytes before (blue) and after (red) the application of 10 μM PIP_2. The $V_{0.5}$ and Q_{app} values for the control group are 177.6 ± 5.5 mV and 1.45 ± 0.15, and for the PIP_2 group, they are 192.6 ± 4.5 mV and 1.00 ± 0.06, respectively; $n = 4$.

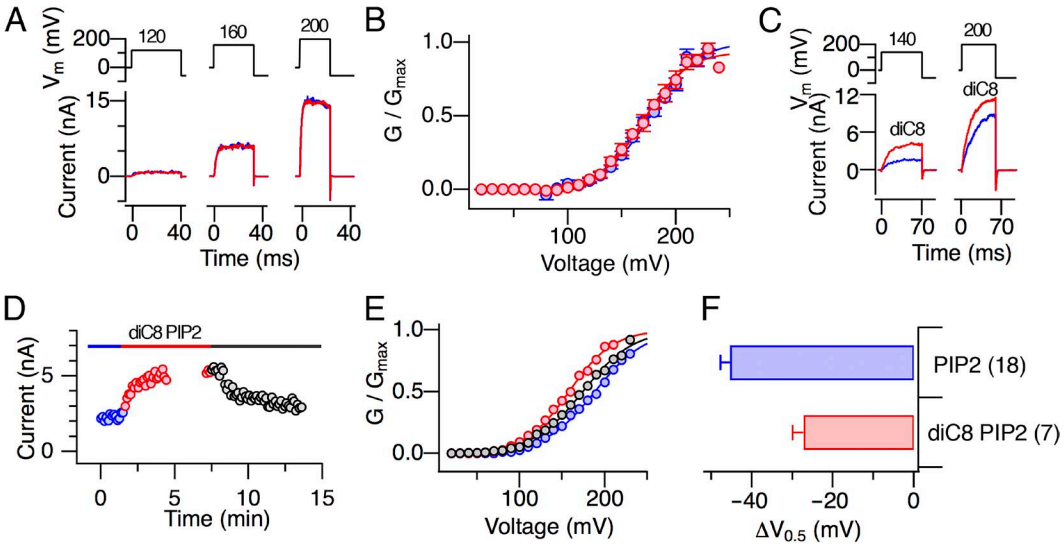

Figure S3. diC8 PIP_2 is less effective than brain-derived PIP_2 on both Slo1 and Slo1 + β1. (A) Representative currents through Slo1 before (blue) and after (red) the application of 10 μM diC8. (B) G-V curves of Slo1 before (blue) and after (red) the application of 10 μM diC8 PIP_2. The smooth curves are Boltzmann fits to the results. The $V_{0.5}$ and Q_{app} values are 168.4 ± 1.8 mV and 1.17 ± 0.06 for control and 173.3 ± 3.8 mV and 1.19 ± 0.06 for the application of diC8 PIP_2 ($n = 6$). (C) Represent currents through Slo1 + β1 before (blue) and after (red) the application of 10 μM diC8. (D) Peak outward currents through Slo1 + β1 elicited by pulses to 120 mV as a function of time. The red bar indicates the diC8 PIP_2 application period. (E) Illustrative Slo1 + β1 G-V curves before (blue), during application of 10 μM diC8 PIP_2 (red), and after washout (black). The $V_{0.5}$ and Q_{app} values are 188 mV and 0.84 for the control group, 158 mV and 0.95 for the PIP_2 group, and 174 mV and 0.84 for the washout group, respectively. (F) Comparison of $\Delta V_{0.5}$ in Slo1 + β1 by 10 μM of brain-derived PIP_2 (blue) and 10 μM diC8 PIP_2 (red). All results shown were obtained without Ca^{2+}. Error bars represent mean ± SEM.

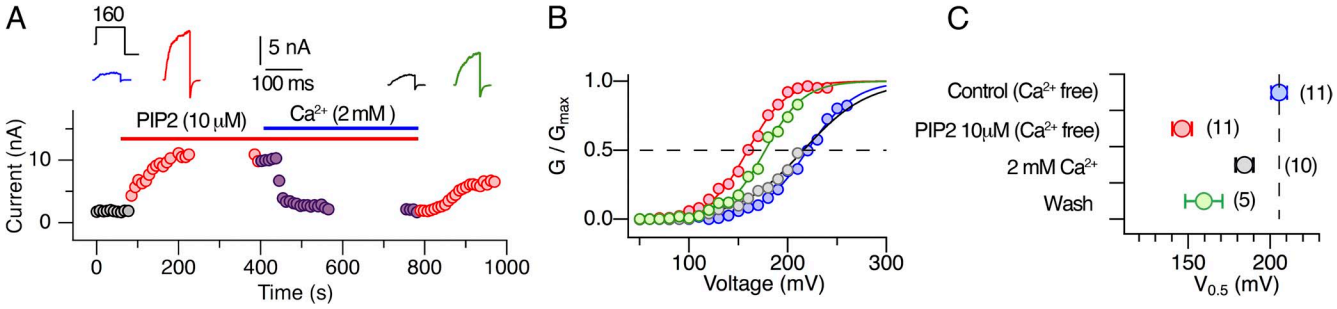

Figure S4. A high concentration of Ca^{2+} antagonizes the stimulatory effect of PIP_2 on Slo1 D362A:D367A:E399A:Δ894–895 + β1. (A) Peak outward currents through Slo1 D362A:D367A:E399A:Δ894–895 + β1 elicited by pulses to 160 mV. The application of 2 mM Ca^{2+} to the intracellular side antagonizes the stimulatory effect of 10 μM PIP_2, and the antagonistic effect of Ca^{2+} is relieved by the Ca^{2+} chelator EGTA (11 mM). (B) Illustrative G-V curves from a patch expressing Slo1 D362A:D367A:E399A:Δ894–895 + β1 channels. Blue, control; red, 10 μM PIP_2; gray, 10 μM PIP_2 + 2 mM Ca^{2+}; green, wash. Similar results were obtained in 10 patches all together ($\Delta V_{0.5} = -15.7 \pm 4.2$ mV). (C) Changes in $V_{0.5}$ by PIP_2, PIP_2 + Ca^{2+}, and wash. Error bars represent mean ± SEM.

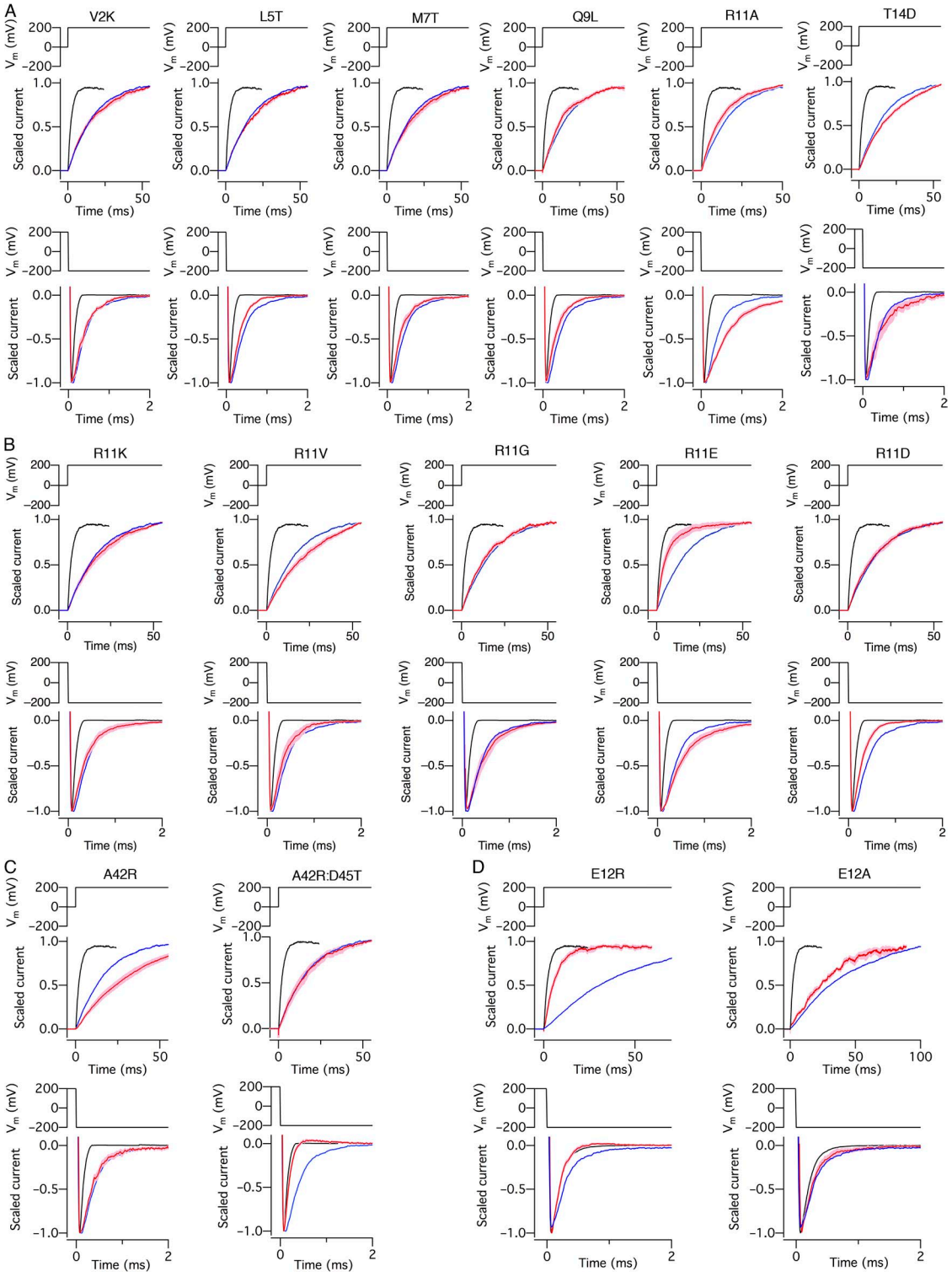

Figure S5. Scaled currents through Slo1 complexes with auxiliary subunits with point mutations. (A) Scaled currents at 200 (top) and −200 mV (bottom) from Slo1 + β1 with β1-to-β2 point mutations (red). For each mutant, the currents obtained from Slo1 alone (black) and Slo1 + wild-type β1 (blue) are shown for comparison. (B) Scaled currents at 200 (top) and −200 mV (bottom) in Slo1 + β1 with mutations at position 11. For each mutant, the currents obtained from Slo1 alone (black) and Slo1 + wild-type β1 (blue) are shown for comparison. (C) Scaled currents at 200 (top) and −200 mV (bottom) in Slo1 + β2 Δ2–32 with β2-to-β1 point mutations (red). For comparison, scaled currents from Slo1 alone (black) and Slo1+ wild-type β2 Δ2–32 (blue) are shown. (D) Scaled currents at 200 (top) and −200 mV (bottom) in Slo1 + β4 with β4-to-β1 point mutations (red). For comparison, scaled currents from Slo1 alone (black) and Slo1 + wild-type β4 (blue) are shown. The sweep width represents mean ± SEM; n = 4–12. All results were obtained without Ca^{2+}.

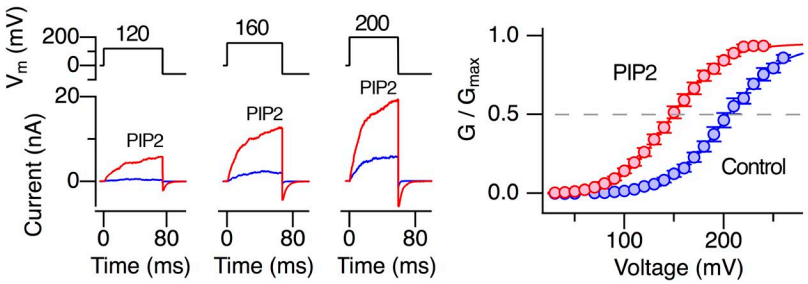

Figure S6. PIP_2 enhances currents through divalent-insensitive Slo1+β1 channels. (A) Representative currents through Ca^{2+}- and Mg^{2+}-insensitive Slo1 D362A:D367A:E399A:Δ894–895 + β1 channels before and after the application of 10 µM PIP_2. (B) G-V curves in Slo1 D362A:D367A: E399A:Δ894–895 + β1 channels before (blue) and after (red) the application of 10 µM PIP_2. The curves represent Boltzmann fits with $V_{0.5}$ = 201.8 ± 2.1 mV and Q_{app} = 1.03 ± 0.05 (Control), and $V_{0.5}$ = 148.5 ± 1.4 mV and Q_{app} = 1.02 ± 0.05 (10 µM PIP_2); n = 14.